

# HiSST: 4th International Conference on High-Speed Vehicle Science Technology 22 -26 September 2025, Tours, France



# Polar Curve Method in Detonation Wave Reflection

Haoran Yan<sup>1</sup>, Ruofan Qiu<sup>2</sup>, Yancheng You<sup>3</sup>

### Abstract

In this study, a modified polar curve method is proposed by incorporating the internal structure of the detonation wave. The result shows that the modified method can address planar and asymmetric ODW reflection, shock wave/detonation wave interactions, and dual solution domain issues. Secondly, it is found that behind the reflected wave and ahead of the expansion fan generated at the wedge trailing edge, the combustion zone, reverse reaction zone, and expansion zone coexist. The shape of the slip line (SL) is found to be more complex than that in typical shock wave flow fields. By adjusting the location where the expansion/shock wave acts, it is shown that this complex flow behavior can affect both the height of the Mach stem (MS) and the stability of the dual solution domain. Finally, the formation mechanisms of the different flow regions are analyzed, and the effects of chemical reactions on flow parameters and SL deflection are investigated.

Keywords: Oblique detonation wave; Mach reflection; Shock wave/detonation wave interaction

# **Nomenclature**

Latin
ODW – Oblique detonation wave
SL – Slip line
RR – Regular reflection
MR – Mach reflection
MS – Mach stem

TP – Triple point

Greek

 $\theta-$  Flow deflection angle Superscripts T - Theoretical value Subscripts cfd - Numerical simulation

fr – Fozen chemistry eq – Chemical equilibrium

# 1. Results and discussions

#### 1.1. Improved Polar Curve Method

When the detonation wave reflects, the resulting flow field is shown in Fig. 1. Since the post-wave flow is supersonic, the incident detonation wave angle remains unaffected by the reflection, allowing the use of the chemical equilibrium limit solution. Most importantly, the post-wave parameters derived under the chemical equilibrium assumption become invalid in this context. Moreover, MR is a key feature of supersonic flow fields. In shock wave flow fields, the height of the MS is typically negatively correlated with the Mach number [1, 2]. However, in the detonation flow field, chemical reactions have a non-negligible influence on the height of the MS. In Fig. 1(a) and Fig. 1(b), as the velocity increases, the Mach number rises from 3.6 to 4.5, and the height of the MS significantly decreases. In contrast, in Fig. 1(c) and Fig. 1(d), the Mach number also increases from 3.6 to 4.5 due to a decrease in temperature,

HiSST-2025-210 Polar Curve Method in Detonation Wave Reflection

<sup>&</sup>lt;sup>1</sup> School of Aerospace Engineering, Xiamen University, Xiamen 361005, China, haoran.yan@stu.xmu.edu.cn

<sup>&</sup>lt;sup>2</sup> School of Aerospace Engineering, Xiamen University, Xiamen 361005, China, rf\_qiu@xmu.edu.cn

<sup>&</sup>lt;sup>3</sup> School of Aerospace Engineering, Xiamen University, Xiamen 361005, China, yancheng.you@xmu.edu.cn

yet the MS height slightly increases. These observations demonstrate that under the same Mach number, variations in inflow conditions can markedly influence the structure of MR. This highlights the importance of thoroughly investigating detonation wave reflection phenomena.

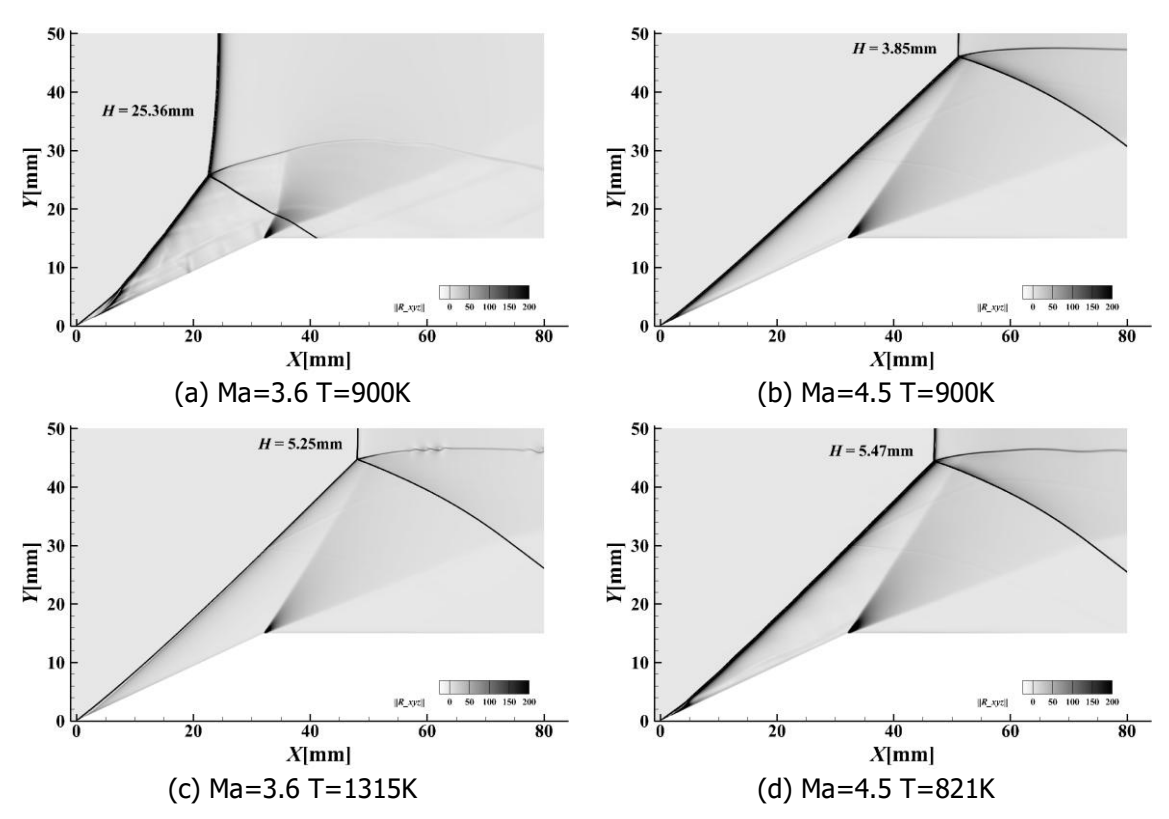


Fig 1. Effect of velocity and temperature variations on the reflection structure.

The two-shock/three-shock theory proposed by von Neumann forms the foundation for solving shock wave reflection problems. Under the conditions of Case 1, Fig. 2 illustrates the typical approach for solving the three-shock theory. This method assumes that the post-wave chemical reaction behind the ODW reaches equilibrium instantaneously and that the reflected wave is an inert shock that does not trigger further chemical reactions [3, 4]. The detonation polar curve intersects with the shock polar curve, yielding a deflection solution denoted as  $\theta^{\Gamma}$ =14.05°. However, numerical simulations indicate that the flow deflection angle at the triple-point location is  $\theta_{\rm cfd}$ =25.6°, which shows a clear discrepancy from the result predicted by the polar method. This suggests that the conventional polar curve approach is flawed and fails to represent the actual flow behavior.

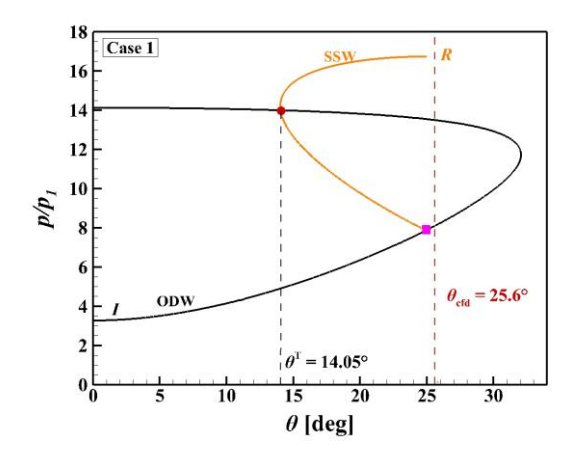


Fig 2. Error of the typical method in solving the three-shock theory.

The primary source of deviation lies in the assumption that the detonation wave is treated as a discontinuity with negligible thickness, just like the shock wave. A real detonation wave is not a

discontinuous surface but has a complex internal structure [5–7]. Similar to the ZND structure, the triple point is connected to the leading shock, followed by a relatively short induction and reaction zone behind the NDW, while the reaction zone behind the ODW is much longer. Near the triple point, chemical reactions cannot reach equilibrium instantly. The polar curve shown in Fig. 2 neglects the lengths of the induction and reaction zones and treats both the shock and detonation waves as discontinuities. In reality, combustion continues downstream of the triple point, and the inflow conditions for the reflected wave are not simply the equilibrium state of region 1.

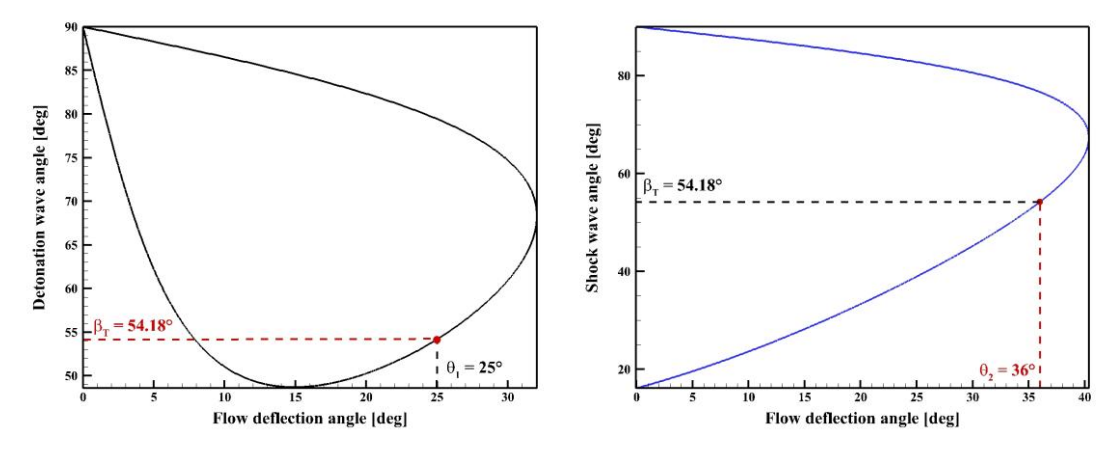


Fig 3. Flow deflection angle of the leading shock.

Based on the above considerations, two limiting cases are assumed: the equilibrium flow assumption and the frozen flow assumption. The equilibrium flow assumption implies that chemical reactions reach equilibrium immediately after passing through the leading shock near the triple point. The frozen-flow assumption implies that chemical reactions have not yet started near the triple point. In essence, this assumption corresponds to solving the polar curve of the leading shock. The wave angle of the leading shock corresponds to the detonation wave angle rather than the shock wave angle induced by the wedge. Based on this principle, Fig. 3 presents the method for determining the flow parameters behind the leading shock. Based on these two assumptions, the polar curves corresponding to the flow field in Fig. 1 can be constructed, as shown in Fig. 4. Curve I<sub>1</sub> represents the chemically equilibrated ODW polar curve, and starting from the corresponding point at a 25° wedge angle, the polar curve of the reflected wave  $R_1^{eq}$  is drawn.  $R_1^{eq}$  is not the inert shock polar curve, but rather a solution based on the equilibrium limit that considers the reverse reactions induced by the reflected wave. The intersection point of  $I_1$  and  $R_1^{eq}$  corresponds to the initial angle of the SL at the triple point under the equilibrium flow assumption, denoted as  $\theta_{\rm eq}$ . Curve  $I_2$  represents the polar curve of the leading shock. The postwave flow deflection angle does not match the 25° wedge angle, but corresponds to the wave angle induced by the ODW generated by the 25° wedge, as shown in Fig. 5. The reflected shock polar curve  $R_2^{\text{fr}}$  is then constructed to intersect with  $I_2$ , yielding the initial angle  $\theta_{\text{fr}}$  of the SL at the triple point under the frozen flow assumption.  $\theta_{\rm eq}$  and  $\theta_{\rm fr}$  are regarded as the upper and lower theoretical bounds of the initial deflection angle  $\theta_{\mathrm{cfd}}$  of the SL at the triple point. When the inflow condition is closer to a singlepeaked model, the measured  $\theta_{cfd}$  in the flow field tends to approach  $\theta_{eq}$ . Otherwise, it is closer to  $\theta_{fr}$ . The values of  $\theta_{\rm cfd}$  are marked in Fig. 4 in red dash line, and it can be observed that, under all four inflow conditions,  $\theta_{cfd}$  is very close to the frozen flow assumption result  $\theta_{eq}$ . This indicates that, under realistic conditions, the frozen flow assumption can be used to approximate  $\theta_{cfd}$ .

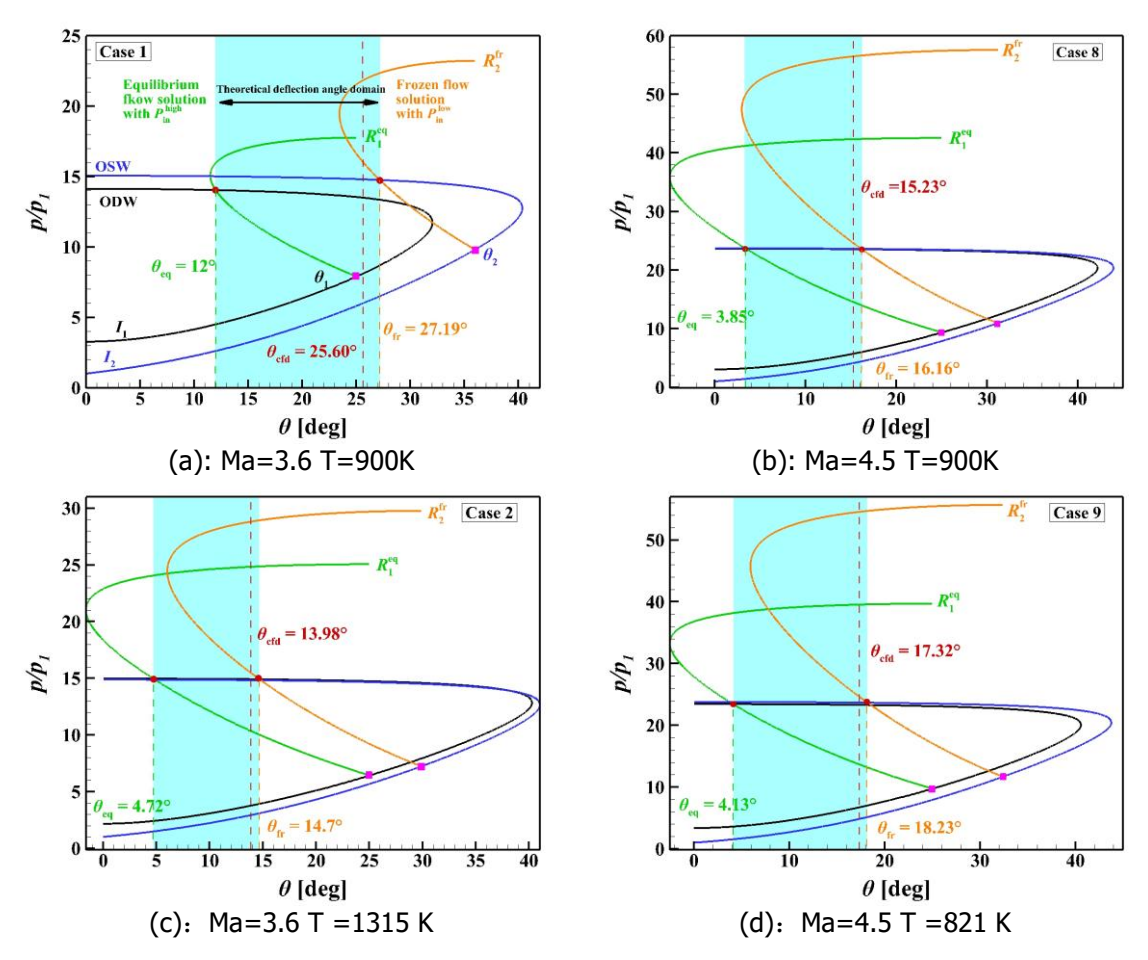
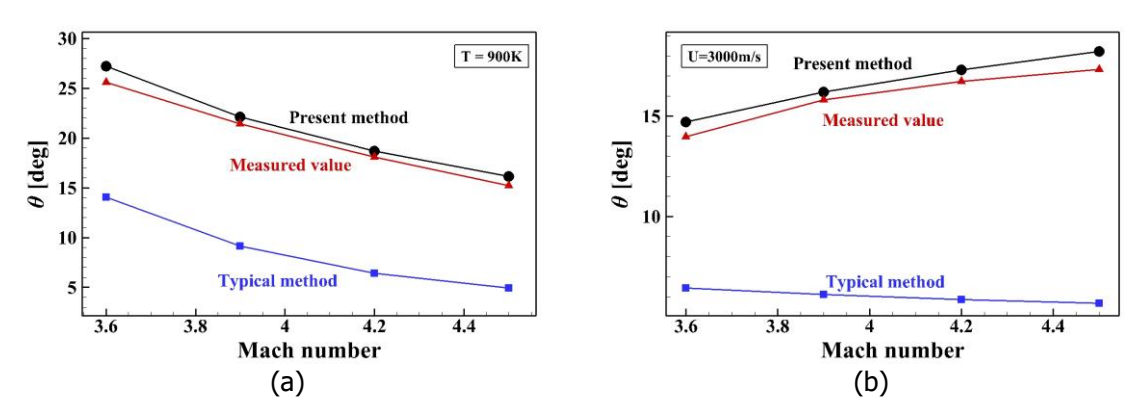


Fig 4. Polar curves under equilibrium and frozen flow assumption.

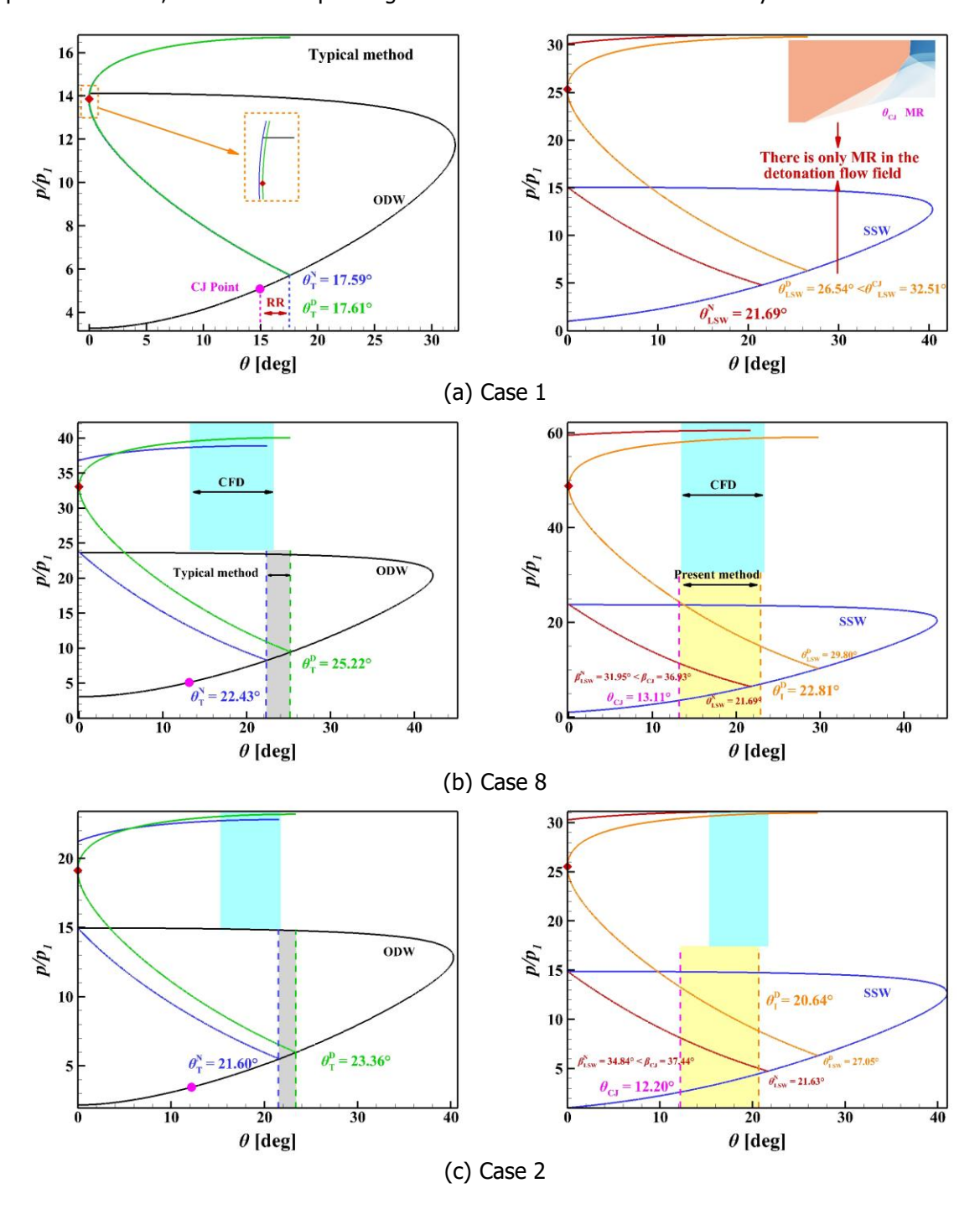
To more intuitively demonstrate the effectiveness of the present method in solving the three-shock theory, Fig. 5 presents a comparison of the initial SL deflection angles obtained by the typical method, the present method, and numerical simulation. In Fig. 5(a), as the velocity increases,  $\theta_{\rm fr}$  and  $\theta_{\rm cfd}$  remain closely aligned. Although the typical method captures the general trend of  $\theta_{\rm cfd}$ , its deviation from the numerical result is significant. In Fig. 5(b), as the temperature decreases, both  $\theta_{\rm fr}$  and  $\theta_{\rm cfd}$  show an upward trend and remain numerically close. However, the typical method yields a downward trend. In addition to producing large numerical errors, the typical method fails to capture the correct variation of  $\theta_{\rm cfd}$ . This further demonstrates that the typical method, which ignores the detonation wave structure, cannot accurately describe the flow near the triple point in ODW flow fields.



**Fig 5.** Comparison of typical method, present method, and numerical simulation: (a) varying velocity; (b) varying temperature.

Now, we apply this finding to the analysis of the dual solution domain. Fig. 6 presents the ODW planar reflection dual solution domains under the four inflow conditions shown in Fig. 1. The left panel uses

the typical method, with the resulting dual solution domain shown in gray, while the blue region represents the dual solution domain obtained from numerical simulations. The right panel uses the present method, and the corresponding dual solution domain is indicated in yellow.



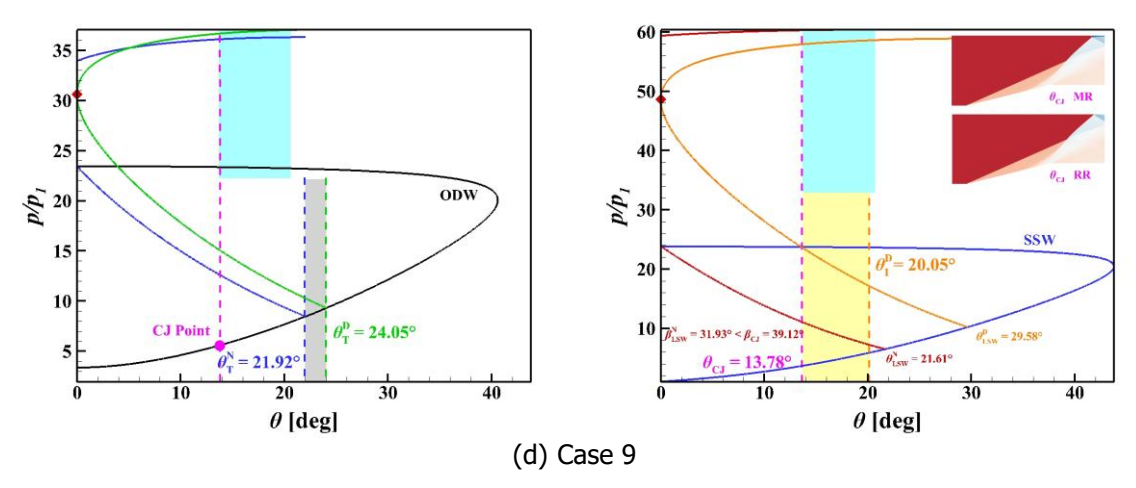


Fig 6. Dual solution domains solved by the typical method (left) and the present method (right).

The typical method exhibits a significant delay in identifying the transition boundary. Specifically, the results based on the equilibrium-limit assumption predict that MR occurs at a much larger wedge angle. In contrast, the present method maintains the error within a reasonable range, and the computed detachment criterion closely matches the actual transition. In practice, the transition from RR to MR occurs at a wedge angle greater than that predicted by the von-Neumann criterion. If it is reasonable to approximate the three-shock theory using the frozen assumption (as validated in the detachment reiterion), there should be some reason why MR near the von-Neumann criterion becomes unstable. It is suspected that this may be because the von-Neumann criterion neglects the influence of the downstream region behind the MS, and thus fails to accurately capture the actual transition point [8]. This downstream influence will be discussed in detail in the next Section.

We then extend the analusis from plannar detonation wave reflection to more complex reflection problems. Fig. 7 presents a flow field involving shock wave/ detonation wave interaction within the dual solution domain. Fig. 8 shows the polar curves obtained using the typical method and the present method, respectively. In Fig. 8(a),  $I_1$  represents the polar curve of the upper incident shock wave in Fig. 7, with a wedge angle of  $10.2^{\circ}$ . The reflected wave of the incident shock is a detonation wave, and  $R_1$  corresponds to the detonation polar curve.  $I_2$  represents the polar curve of the lower incident ODW, with a wedge angle of  $23^{\circ}$ .  $R_2$  denotes the polar curve of the shock wave reflected from the detonation wave. When the flow field exhibits regular reflection, the intersection of the weak solutions of polar curves  $R_1$  and  $R_2$  corresponds to the solution at TP0 in Fig. 7(a). When the flow field exhibits MR, the intersection of  $R_1$  and  $R_2$  corresponds to TP1 in Fig. 7(b), and the intersection of  $R_2$  and  $R_3$  corresponds to TP2 in Fig. 7(b).

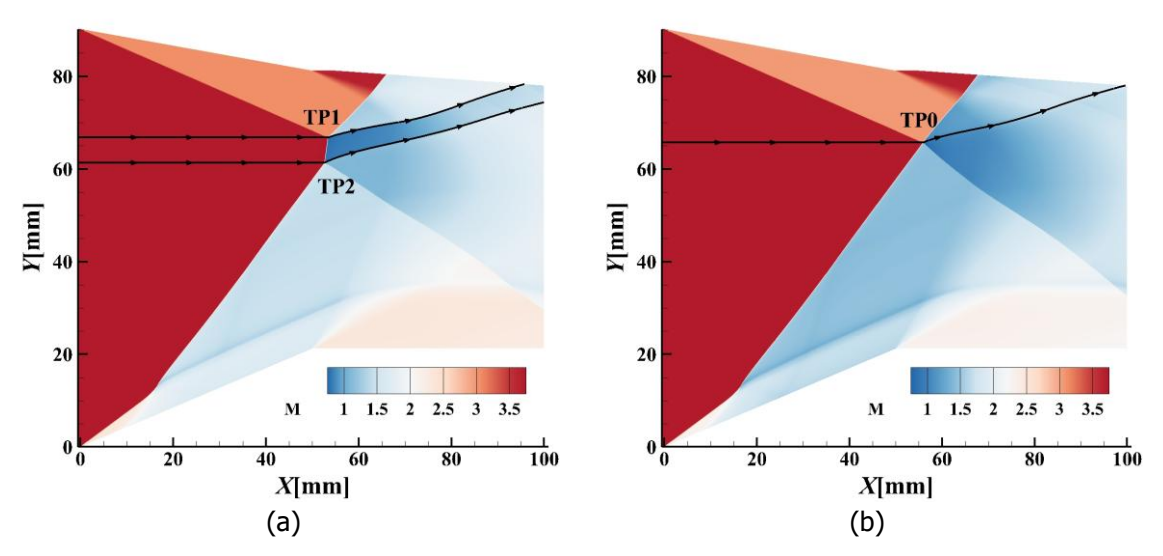
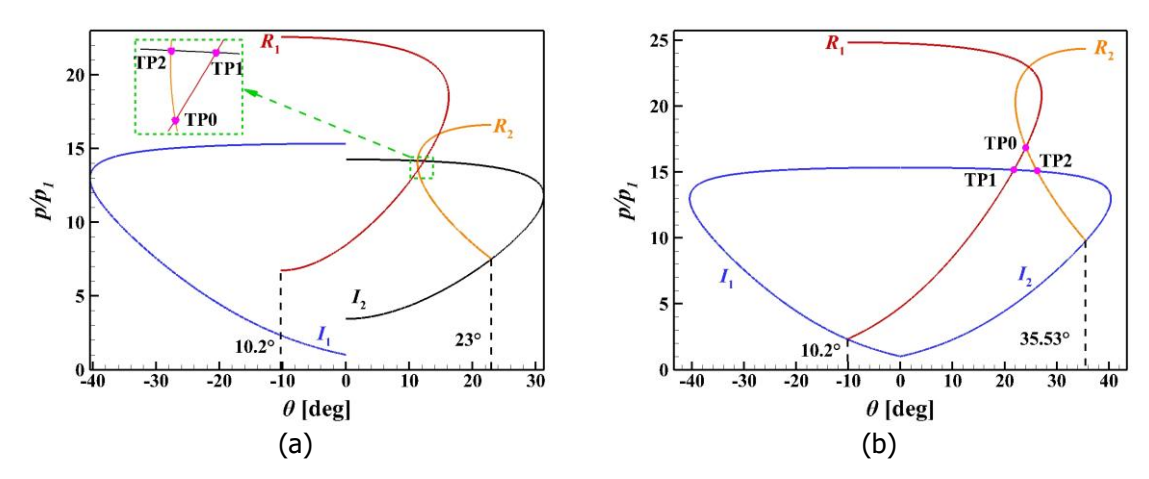


Fig 7. Dual solution flow fields of shock wave/detonation wave interaction: (a) RR (b) MR.



**Fig 8.** Polar curves of shock wave/detonation wave interaction: (a) typical method; (b) present method.

Fig. 9 illustrates the dual solution flow field of asymmetric ODW reflection, and Fig. 10 shows the polar curves generated by the two solution methods. The resulting oMR structures differ between the two methods, and there is a clear difference in the post-reflection pressure of the RR. In the typical method, both  $\rm I_1$  and  $\rm I_2$  are detonation wave polar curves based on the chemical equilibrium limit, while  $\rm R_1$  and  $\rm R_2$  correspond to inert shock waves. The typical method yields an oMR structure composed of an InMR and a DiMR, with a post-wave pressure ratio of approximately 20. In contrast, the present method uses the polar curve of the leading shock wave corresponding to the detonation wave angle, and predicts an oMR structure consisting of two DiMRs, with a post-wave pressure ratio of about 40.

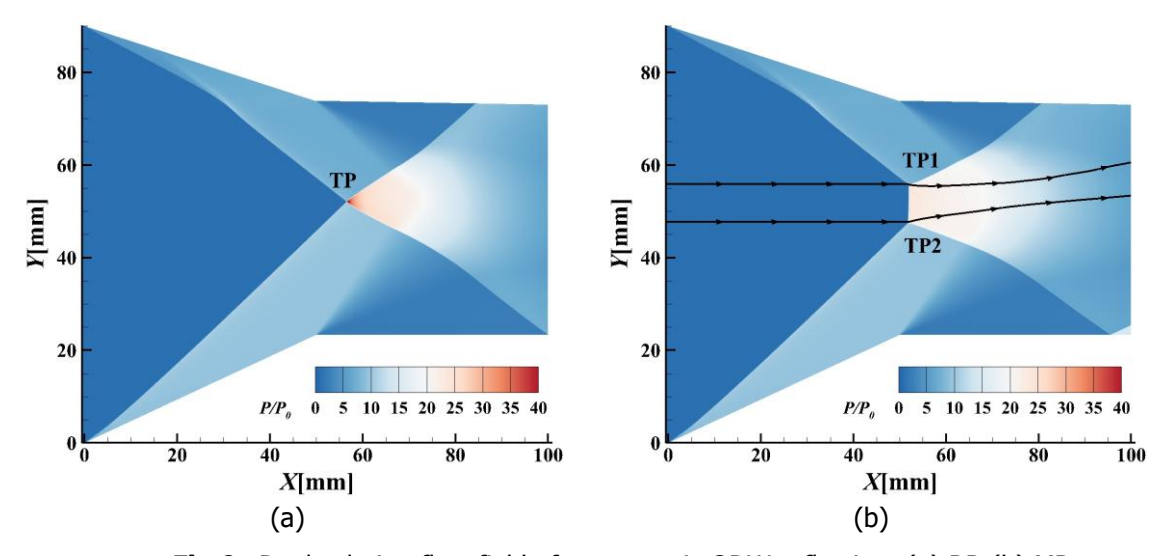


Fig 9. Dual solution flow field of asymmetric ODW reflection: (a) RR (b) MR.

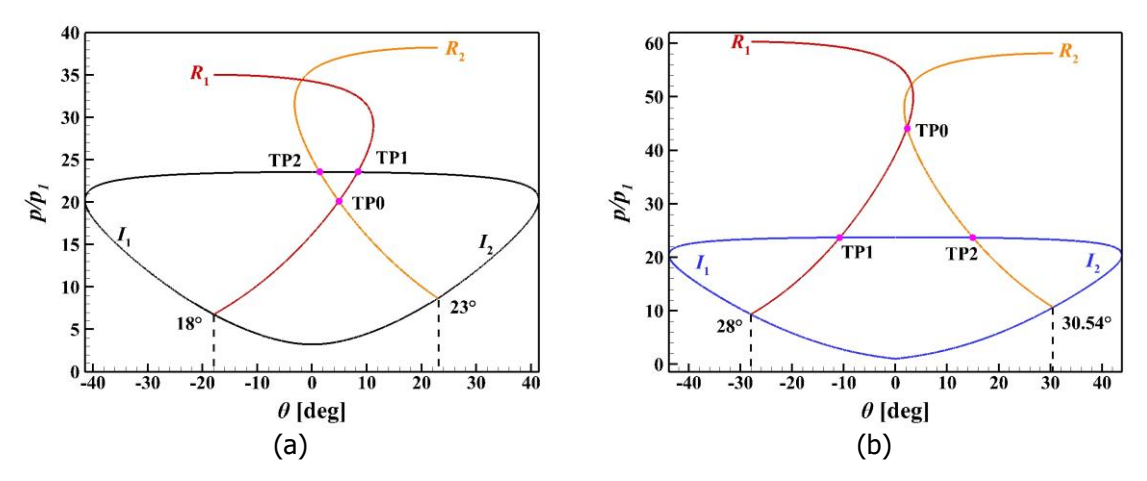
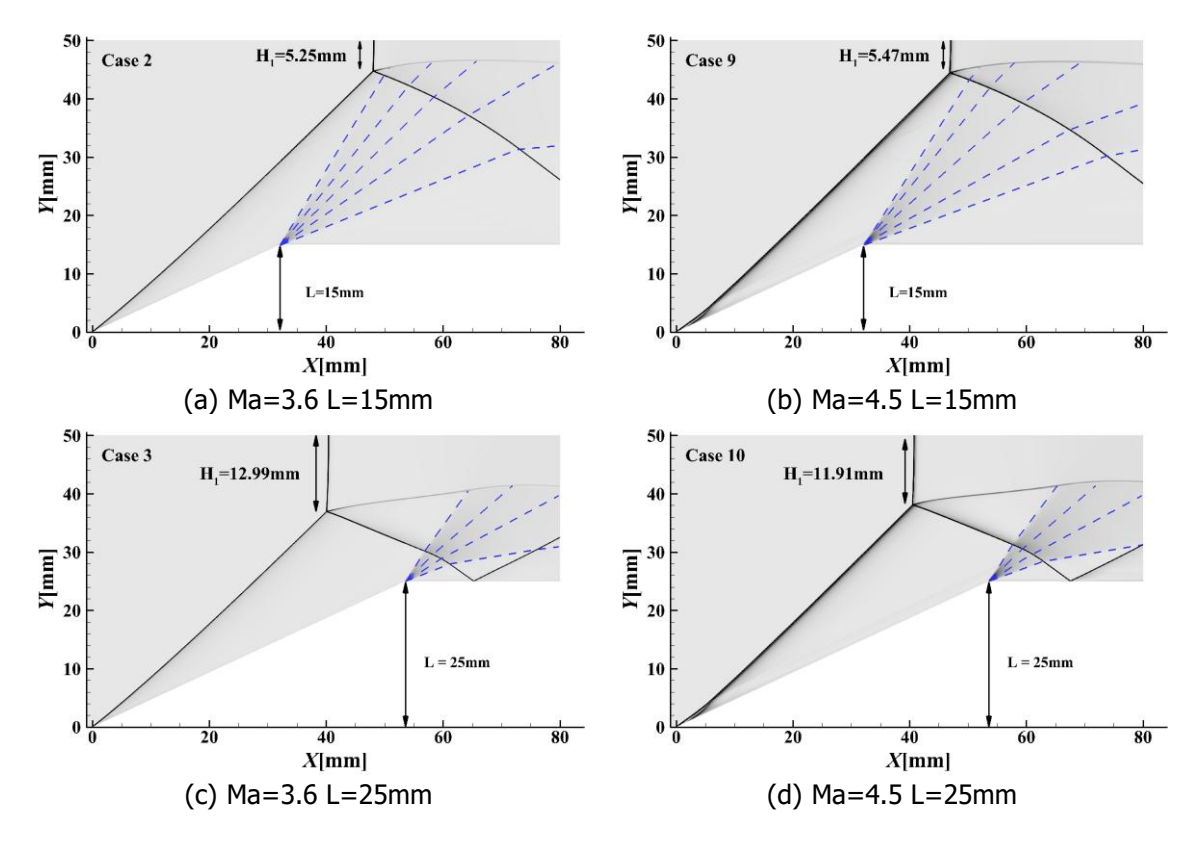


Fig 10. Polar curves of asymmetric ODW reflection: (a) typical method (b) present method.

## 1.2. Flow details behind the reflected wave

To demonstrate that the downstream flow from the triple point may influence the MR structure, Fig. 11 presents the effect of Mach number and wedge length on the movement of the MS. In Figs. 11(a) and 11(b), the expansion wave acts near the leading edge of the SL, and the flow behind the reflected wave is entirely covered by the expansion fan. Under this condition, increasing the Mach number leads to an increase in MS height. When the expansion fan acts farther downstream, as in Figs. 11(c) and 11(d), a longer wedge shifts its influence to the trailing end of the SL, and increasing the Mach number instead reduces the MS height. Furthermore, Section 1.1 shows that Mach reflection becomes unstable near the von-Neumann criterion, which is particularly evident in Fig. 12(c). Numerical results indicate that the RR-to-MR transition occurs at a wedge angle of 15.5°. Fig. 12(a) shows a stable RR at a 15° wedge, which remains unchanged even under imposed perturbations. In contrast, Fig. 12(b) introduces a second wedge to generate a shock downstream of the reflection point, enabling the flow field to stabilize in an MR configuration. This indicates that there is a complex flow interaction between the post-reflection flow and the expansion fan. Such flow details affect the movement of the MS and the stability of the dual solution domain.



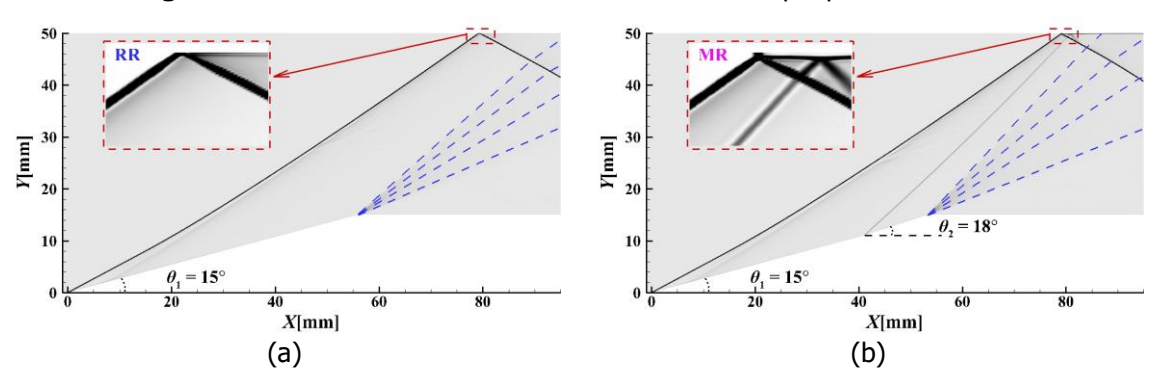


Fig 11. The Influence of downstream flow from the triple point on MS movement.

Fig 12. Effect of downstream flow on the stability of MR within the dual solution domain.

After a series of analyses, we coonsider that the reflection of an ODW is neither a simplified interaction between energy-releasing shock waves nor an idealized interaction between leading shocks under equilibrium conditions. Instead, it involves more complex issues such as the spatially nonuniform distribution of the reaction zone and the shifting of chemical equilibrium. Based on these insights, Fig. 13 illustrates a schematic of the planar reflection flow field of an ODW, focusing on the post-reflection flow and the shape of the SL. Region (2) represents the reverse reaction zone that forms after the hydrogen is fully combusted and then passes through the reflected wave. Region (3) corresponds to the area where hydrogen is not fully combusted and continues to burn after passing through the reflected wave. This region is relatively small, and secondary compression waves are generated along the SL to balance the pressure difference between the two sides. Region (4) is the area where the SL provides expansion; the inflection point of the SL turning angle should lie downstream of the expansion onset because it should counteract the streamline deflection caused by the reverse reaction zone. Finally, based on the analysis of the post-reflection flow, the Von-Neumann criterion discussed in Section 1.1 is revisited. The three-shock theory does not account for the influence of downstream flow. When solving the Von Neumann criterion, it is assumed that the initial turning angle of the SL is zero, representing the limiting condition for the occurrence of MR. However, due to the downward deflection of the SL in Region (3), a contracting subsonic duct cannot form, rendering the MR structure unstable. Therefore, the actual transition from RR to MR occurs at a certain point within the dual solution domain.

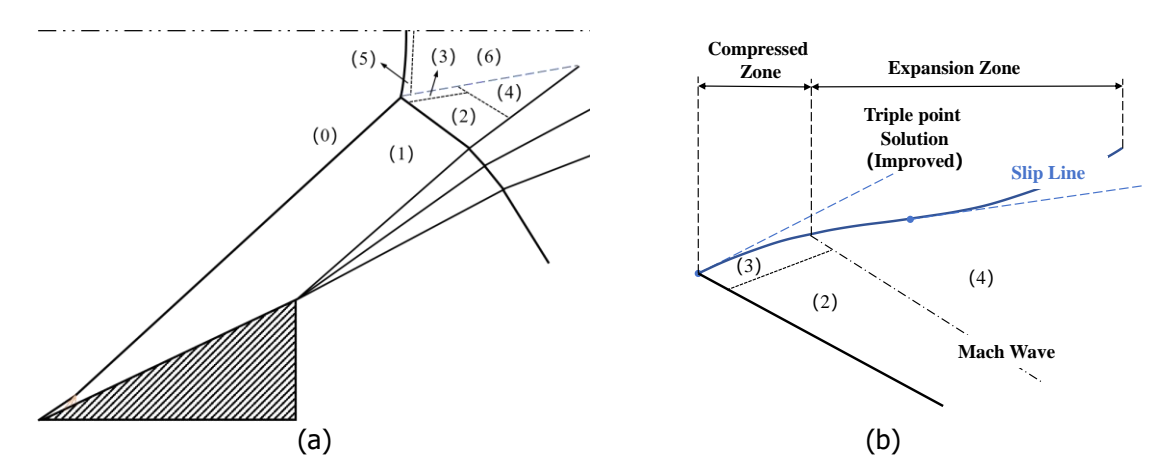


Fig 13. (a) Schematic of oblique detonation reflection structure (b) Schematic of SL shape.

## References

- 1. Azevedo, D.J., Liu, C.S.: Engineering Approach to the Prediction of Shock Patterns in Bounded High-Speed Flows, American Institute of Aeronautics and Astronautics Journal 31, 83-90 (1993)
- 2. Li, H., Ben-Dor, G.: A parametric study of Mach reflection in steady flows, Journal of Fluid Mechanics 341, 101-125 (1997)

- 3. Zhang, Z.J., Liu, Y.F., Wen, C.Y.: Formation of stabilized oblique detonation waves in a combustor, Combustion and Flame 223, 423-436 (2021)
- 4. Sun, J., Yang, P.F., Chen, Z.: Dynamic interaction patterns of oblique detonation waves with boundary layers in hypersonic reactive flows, Combustion and Flame 271, 113832 (2025)
- 5. Zeldovich Y.B.: On the theory of the propagation of detonation in gaseous systems, Technical Report Archive and Image Library 10, 542-568 (1940)
- 6. Von Neumann, J.: Theory of detonation waves, Collected Works of John von Neumann (1942)
- 7. Döering, W.: On detonation processes in gases, Annuals of Physics 435, 421-436 (1943)
- 8. Zhang, T., Xu, K., et al.: Reflection and transition of planar curved shock waves, Journal of Fluid Mechanics 959, A11 (2023)